Drag coefficient of a gas bubble in an axisymmetric shear flow

S. Takagi[a] and A. Prosperetti
Department of Mechanical Engineering, The Johns Hopkins University, Baltimore, Maryland 21218

Y. Matsumoto
Department of Mechanical Engineering, University of Tokyo, Bunkyo-ku, Tokyo 113, Japan

(Received 16 November 1993, accepted 25 April 1994)

The drag coefficient of a gas bubble in steady motion in an unbounded axisymmetric shear flow is obtained numerically for different values of the Reynolds and Weber numbers.

Ryskin and Leal used a novel boundary-fitted coordinate generation method[1] to study the flow around a bubble rising at constant velocity in a quiescent, unbounded viscous liquid.[2–4] They allowed the shape of the bubble surface to adjust to the flow so that the kinematic and dynamic boundary conditions could be exactly satisfied. They also assumed that the gas–liquid interface was free of impurities, so that zero-tangential-stress boundary conditions applied.

In the present study we extend their results to the case in which the fluid far from the bubble is not at rest, but in a state of uniform axisymmetric shear with the axis coincident with the symmetry axis of the bubble. We use a recent extension of their numerical technique described in Ref. 5. Other slight differences with their numerical approach are described at the end of this note.

In addition to its intrinsic fluid dynamic interest, the present study is relevant for the understanding of the flow of bubbly liquids, in which bubbles typically move in regions of nonuniform flow. While the present axisymmetric flow is certainly a very special case, it is relatively simple to analyze and gives some indication on the behavior of the drag coefficient in response to disturbances of the incoming flow.

Consider an axisymmetric shear flow given, far from the bubble, by

$$u=U-\tfrac{1}{2}\Omega r^2, \quad v=0. \tag{1}$$

Here u and v are the velocity components respectively parallel and orthogonal to the axis (taken as the x axis and oriented in the direction of U), and r is the distance from the axis. In the frame of reference of the bubble, U is the constant velocity attained under the action of a constant prescribed force such as buoyancy, and Ω is a parameter related to the magnitude of the shear. The velocity field (1) is an exact solution of the Navier–Stokes equations with a pressure field given by

$$\frac{\partial p}{\partial x}=-2\mu\Omega, \tag{2}$$

where μ is the viscosity. The associated streamfunction ψ and vorticity field ω are given by

$$\psi=\tfrac{1}{2}r^2(U-\tfrac{1}{4}\Omega r^2), \quad \omega=r\Omega. \tag{3}$$

The inviscid flow generated by spheres and ellipsoids immersed in the flow field (1) has been studied by Rubel.[6]

We solve the Navier–Stokes equations imposing that the flow is given by (1) far from the bubble and that the usual kinematic and dynamic boundary conditions hold at the bubble surface, including the effect of surface tension. In the following we use quantities made dimensionless with respect to the equivalent bubble radius a and the velocity U. The nondimensionalization of the equations introduces the Reynolds and Weber numbers

$$\mathrm{Re}=2aU\rho/\mu, \quad \mathrm{We}=2\rho aU^2/\sigma, \tag{4}$$

and the shear parameter

$$\Omega_*=a^2\Omega/U. \tag{5}$$

Here ρ and σ are the liquid density and interfacial tension. The drag coefficient is defined in the usual way by

$$C_D=F/\tfrac{1}{2}\rho U^2\pi a^2, \tag{6}$$

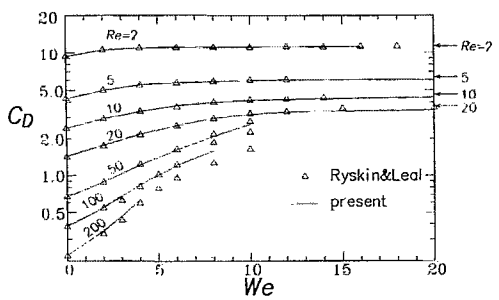

FIG. 1. Drag coefficient for steady motion in a quiescent fluid, $\Omega_*=0$. The lines are the results of Ref. 4, the circles the present ones.

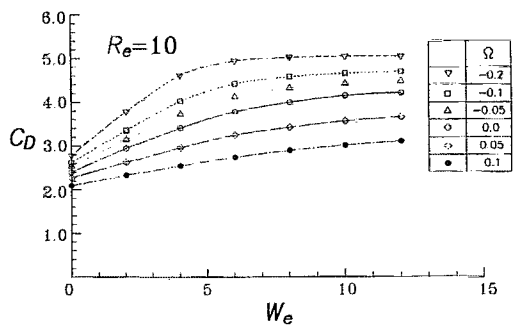

FIG. 2. Drag coefficient as a function of the Weber number for Re=10 and different values of the shear parameter Ω_*.

[a]On leave from Department of Mechanical Engineering, University of Tokyo.

 1070-6631/94/6(9)/3186/3/$6.00

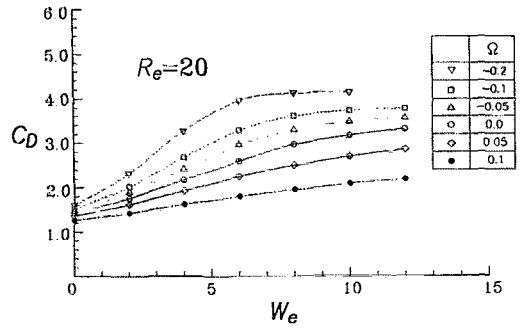

FIG. 3. Drag coefficient as a function of the Weber number for Re=20 and different values of the shear parameter Ω_*.

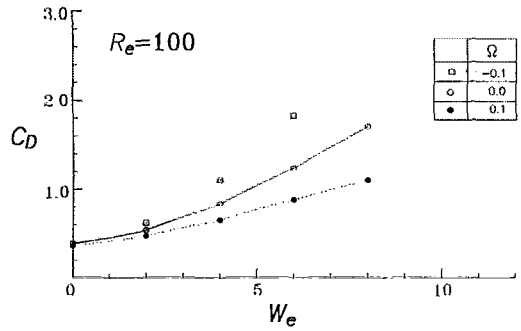

FIG. 4. Drag coefficient as a function of the Weber number for Re=100 and different values of the shear parameter Ω_*.

where F is the total hydrodynamic force acting on the bubble which, in steady conditions, equals the imposed force.

In Fig. 1 we compare our results for $\Omega_*=0$ with those of Ryskin and Leal[3] (triangles). The figure shows the drag coefficient as a function of the Weber number for several Reynolds numbers. The agreement is excellent up to Re=50. For Re=100 and 200 the present results are slightly different from those of Ryskin and Leal possibly due to the alternative coordinate generation method that we use.

The effects of shear for Re=10, 20 and 100 are demonstrated in Figs. 2–4, in which C_D is shown as a function of We for different values of Ω_*. To interpret these results it is useful to keep in mind that $(1/2)\Omega_*$ is the percent free-stream velocity change at unit distance from the axis of symmetry, so that, for example, $\Omega_*=0.1$ corresponds roughly to a 5% velocity drop over the bubble radius. The magnitude of the effect is thus seen to be quite large, particularly at the larger Weber numbers where the bubble is more highly deformed. It is seen from Fig. 1 that, with increasing We, the drag coefficient reaches an asymptotic value, at least for moderate Reynolds numbers. Figures 2 and 3 show that, for $\Omega_*<0$, the asymptotic value is attained at smaller Weber numbers while, for $\Omega_*>0$, it is reached beyond the range of values of We that we have studied, if at all.

It is also interesting to look at the effect of the free-stream shear on the flow and bubble shape. Figure 5 shows the bubble and the stream lines for Re=20, We=8, and

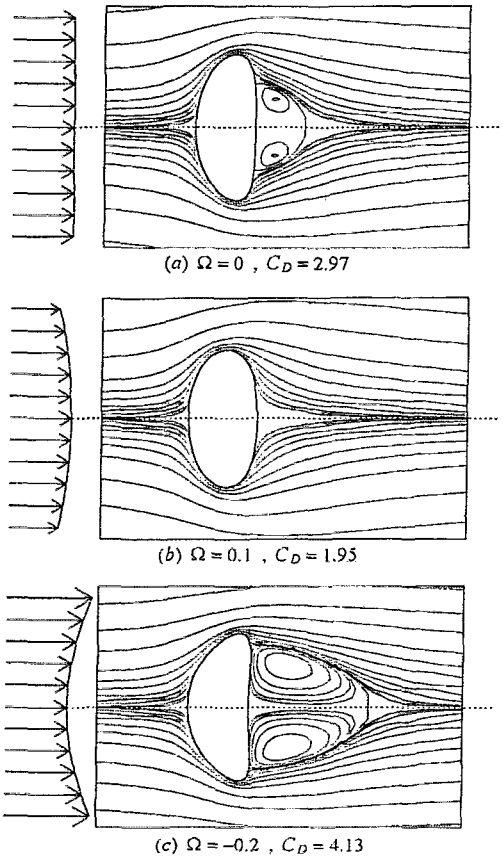

FIG. 5. Computed bubble shape and stream lines for Re=20, We=8, and $\Omega_*=0$ (top), 0.1 (center), and −0.2 (bottom).

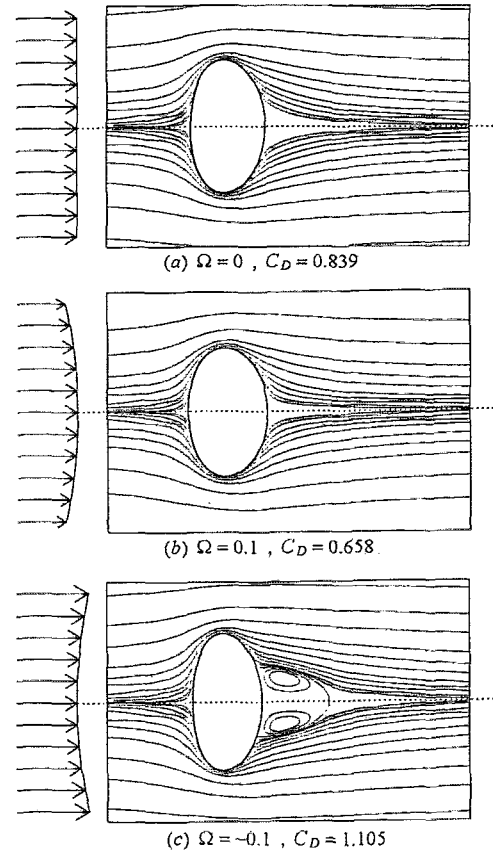

FIG. 6. Computed bubble shape and stream lines for Re=100, We=4, and $\Omega_*=0$ (top), 0.1 (center), and −0.1 (bottom).

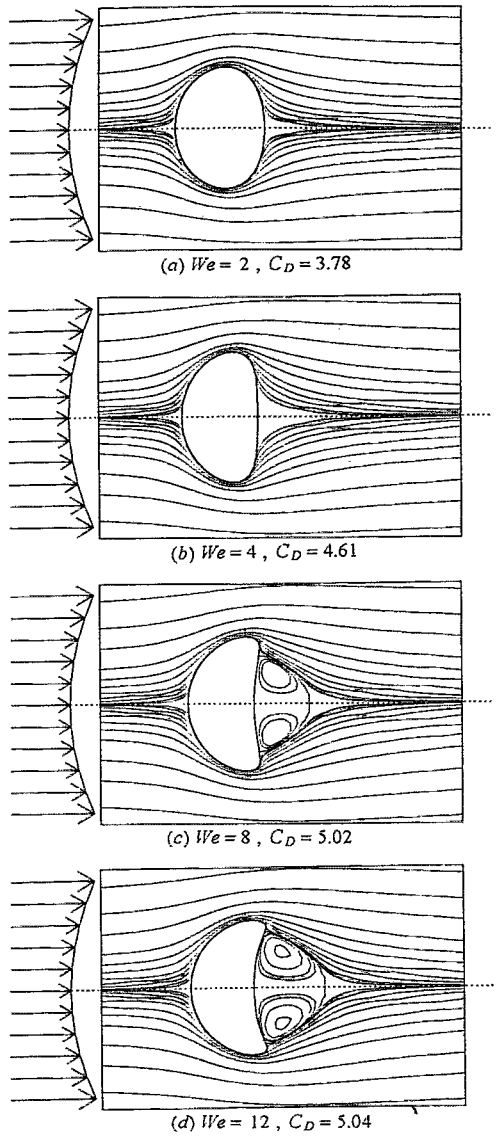

FIG. 7. Computed bubble shapes for Re=10, $\Omega_*=-0.2$, and different values of the Weber number.

$\Omega_*=0$, 0.1, and -0.2. It is seen that a positive shear has a strong tendency to inhibit the recirculating eddy behind the bubble, with a consequent drop of the drag coefficient from 2.97 to 1.95. Conversely, a negative shear considerably increases the attached eddy and, with it, the drag coefficient that reaches the value of 4.13 in this example. A similar trend is observable in Fig. 6 for Re=100. A smaller, but qualitatively similar effect, is also found for smaller We, i.e., less deformable bubbles. The low-Reynolds-number shapes of Fig. 5 show a marked flattening of the rear part of the bubble while, for Re=100 (Fig. 6), the flattening is more pronounced at the front. A comparison among Figs. 2–4 indicates that this difference, which is in keeping with the results of Ref. 3, has little effect on the dependence of C_D on We and Ω, at least in the low-Weber-number region. Figure 7 shows the effect of We on the bubble shape for Re=10 and $\Omega_*=-0.2$.

The referee of this paper suggested that the drag coefficient might depend on the incident flow only indirectly through its effect on the bubble shape. To test this hypothesis we have performed several calculations placing a bubble with the shape determined for a certain value of Ω_* in flows with different Ω_*, including $\Omega_*=0$, i.e., a uniform flow. The drag coefficient was found to be a strong function of Ω_* *for the same bubble shape*. This direct effect of the incident flow is probably mediated by the evolution of the vorticity field around the bubble.

The numerical method we have used is essentially the same as that of Ryskin and Leal with two modifications. First, due to the alternative formulation of the coordinate generation method of Ref. 5, at each iteration we are able to update directly the bubble surface, rather than the metric coefficients as in Refs. 2–4. Thus, using the same notation as in the references, we write

$$x_0^{n+1}=(\tfrac{4}{3}\pi/V^n)^{1/3}x_0^n+\beta\Pi^n(x_1^n-x_0^n), \tag{7}$$

with a similar equation for the radial coordinate. The factor in the first term enforces conservation of the bubble volume and the parameter Π, equal to the normal stress imbalance across the surface, "guides" the surface nodes towards their proper position. The constant β is used for under-relaxation. Secondly, for large values of Re and Ω_*, the undisturbed velocity boundary condition "at infinity" is imposed on an outer boundary in the form of a prolate ellipsoid, rather than a sphere. The major and minor axes of this ellipsoid were taken as 11.5 and 8 bubble radii, respectively.

ACKNOWLEDGMENTS

This study was begun while A.P. was Mitsubishi Visiting Professor at the University of Tokyo's Research Center for Advanced Science and Technology. He wishes to express his deep gratitude to Mitsubishi Heavy Industries LTD for the generous support received and to RCAST and the Department of Mechanical Engineering of the University of Tokyo for their kind hospitality. Subsequent support from NSF under Grant No. CTS-8918144 and DOE under Grant No. DE-FG02-89ER14043 is also gratefully acknowledged. S. T. gratefully acknowledges the support received from the Japan Society for the Promotion of Science through a Fellowship for Junior Japanese Scientists during his stay at the Johns Hopkins University.

[1] G. Ryskin and L. G. Leal, "Orthogonal mapping," J. Comput. Phys. **50**, 71 (1983).
[2] G. Ryskin and L. G. Leal, "Numerical solution of free-boundary problems in fluid mechanics. Part 1. The finite-difference technique," J. Fluid Mech. **148**, 1 (1983).
[3] G. Ryskin and L. G. Leal, "Numerical solution of free-boundary problems in fluid mechanics. Part 2. Buoyancy-driven motion of a gas bubble through a quiescent liquid," J. Fluid Mech. **148**, 19 (1983).
[4] G. Ryskin and L. G. Leal, "Numerical solution of free-boundary problems in fluid mechanics. Part 3. Bubble deformation in an axisymmetric straining flow," J. Fluid Mech. **148**, 37 (1983).
[5] R. Duraiswami and A. Prosperetti, "Orthogonal mapping in two dimensions," J. Comput. Phys. **98**, 254 (1992).
[6] A. Rubel, "Axisymmetric shear flow over spheres and spheroids," AIAA J. **24**, 630 (1986).